Identification of extra neutral gauge bosons at the International Linear Collider

P. Osland,[a,1] A. A. Pankov,[b,2] and A. V. Tsytrinov[b,3]

[a]Department of Physics and Technology, University of Bergen, Postboks 7803, N-5020 Bergen, Norway

[b]The Abdus Salam ICTP Affiliated Centre, Technical University of Gomel, 246746 Gomel, Belarus

Abstract

Heavy neutral gauge bosons, Z's, are predicted by many theoretical schemes of physics beyond the Standard Model, and intensive searches for their signatures will be performed at present and future high energy colliders. It is quite possible that Z's are heavy enough to lie beyond the discovery reach expected at the CERN Large Hadron Collider LHC, in which case only indirect signatures of Z' exchanges may occur at future colliders, through deviations of the measured cross sections from the Standard Model predictions. We here discuss in this context the foreseeable sensitivity to Z's of fermion-pair production cross sections at an e^+e^- linear collider, especially as regards the potential of distinguishing different Z' models once such deviations are observed. Specifically, we assess the discovery and identification reaches on Z' gauge bosons pertinent to the E_6, LR, ALR and SSM classes of models, that should be attained at the planned International Linear Collider (ILC). With the high experimental accuracies expected at the ILC, the discovery and the identification reaches on the Z' models under consideration could be increased substantially. In particular, the identification among the different models could be achieved for values of Z' masses in the discovery (but beyond the identification) reach of the LHC. An important role in enhancing such reaches is played by the electron (and possibly the positron) longitudinally polarized beams. Also, although the purely leptonic processes are experimentally cleaner, the measurements of c- and b-quark pair production cross sections are found to carry important, and complementary, information on these searches.

[1]E-mail: per.osland@ift.uib.no
[2]E-mail: pankov@ictp.it
[3]E-mail: tsytrin@rambler.ru

1 Introduction

Electroweak theories beyond the Standard Model (SM) based on spontaneously broken extended gauge symmetries naturally envisage the existence of heavy, neutral, vector bosons Z'. The variety of the proposed Z' models is somewhat broad, and for definiteness in the sequel we shall focus on the so-called $Z'_{\rm SSM}$, Z'_{E_6}, $Z'_{\rm LR}$ and $Z'_{\rm ALR}$ models. Particular attention has recently been devoted to the phenomenological properties and the search reaches on such scenarios, and in some sense we may consider these Z' models as representative of this New Physics (NP) sector [1, 2].

A typical manifestation of the production of such states is represented by (narrow) peaks observed in the cross sections for processes among SM particles at high energy accelerators, for example in the invariant mass distributions for Drell-Yan dilepton pair production at the Fermilab Tevatron or at the CERN LHC hadronic colliders. Current experimental search limits on $M_{Z'}$ at 95% C.L., from Drell-Yan cross sections at the Tevatron, generally range in the interval 0.8–1 TeV, depending on the particular Z' model being tested [3]. Even higher 95% C.L. limits, of the order of 1.14–1.4 TeV are obtained for the Z'_χ, $Z'_{\rm LR}$, and $Z'_{\rm SSM}$ models, from electroweak high precision data [2].

Clearly, the eventual discovery of a peak should be supplemented by the verification of the spin-1 of the assumed underlying Z', vs. the alternative spin-2 and spin-0 hypotheses corresponding, e.g., to exchanges of a Randall-Sundrum graviton resonance [4] or a sneutrino [5]. This kind of analysis relies on appropriate angular differential distributions and/or angular asymmetries. Finally, once the spin-1 has been established, the particular Z' scenario pertinent to the observed signal should be identified, see, e.g., Refs. [6–15]. From studies of Drell-Yan processes at the LHC with a time-integrated luminosity of 100 fb^{-1}, it turns out that one can expect, at the 5-σ level, discovery limits on $M_{Z'}$ of the order of 4–4.5 TeV, spin-1 identification up to $M_{Z'} \simeq$ 2.5–3 TeV and potential of distinction among the individual Z' models up to $M_{Z'} \simeq 2.1$ TeV (95% C.L.).

For masses above the direct search limits mentioned above, and LHC luminosity at the design value, access to Z' manifestations may be provided by indirect, virtual exchange effects causing deviations of cross sections from the SM predictions, if $M_{Z'}$ is not excessively heavy. However, at the LHC, model identification from Drell-Yan dilepton mass distributions and forward-backward asymmetries may be problematic due to limited statistics [16].

An alternative resource for the observation of virtual heavy gauge boson exchanges should be represented by the next generation e^+e^- International Linear Collider (ILC), with center of mass energy $\sqrt{s} =$ 0.5–1 TeV and typical time-integrated luminosities $\mathcal{L}_{\rm int} \sim$ 0.5–1 ab^{-1} [17,18], and the really high precision measurements that will be possible there. Indeed, the baseline configuration envisages a very high electron beam polarization (larger than 80%). Also positron beam polarization, around 30%, might be initially obtainable and perhaps already available for physics. This polarization could be raised to about 60% or higher in the ultimate upgrade of the machine. The polarization option might represent an asset in order to enhance the discovery reaches and identification sensitivities on NP models of any kind [19], therefore also on Z' exchanges in interactions of SM particles. Previous analyses, based on various final state channels and possible experimental observables, show that sensitivities to quite high Z' masses could in principle be attained at the ILC (qualitatively, of the order of $M_{Z'} \sim (10 - 20) \cdot \sqrt{s}$ for the highest planned luminosity, see, e.g., [1,20–24], and references therein). The ILC parameters have

recently been fixed in the Reference Design Report [17], so that it should be interesting to reconsider the identification of Z' models in the light of the numbers reported there.

We will here focus on the fermion-antifermion production reactions at the polarized ILC:

$$e^+ + e^- \to f + \bar{f}, \qquad f = e, \mu, \tau, c, b. \tag{1}$$

As basic experimental observables for the Z' analysis, as an alternative to integrated observables like the total cross sections and/or angular-integrated asymmetries, we here choose the differential angular distributions for the above processes, that allow to exploit the information contained in the different portions of the final state phase space by a binned analysis. Particular emphasis will be given to the comparison between the cases of unpolarized and polarized initial beams, as regards the expected potential of ILC in identifying the Z' models of interest here, for $M_{Z'}$ values of the order of and beyond the limits accessible at the LHC.

Indeed, concerning the Z' mass, there are two scenarios. The first one is represented by the interval in $M_{Z'}$ between the expected identification and discovery limits at the LHC: here, we can assume the Z' to have already been discovered at some $M_{Z'}$ (but the model not identified), so that the model identification (or equivalently the determination of the coupling constants) could be performed at the ILC, based on the deviations of cross sections from the SM predictions for the determined Z' mass. For earlier attempts along this line see, e.g., Ref. [25]. The second mass range is above the LHC discovery limit and, here, with $M_{Z'}$ unknown, both discovery and identification reaches should be assessed for the ILC.

In the following, in Sec. 2 we give a brief introduction to the different Z' models considered in the analysis, and give the corresponding leading order expressions of the polarized differential cross sections for processes (1), mostly in order to establish the notations. In Secs. 3 and 4 we present the results of our analysis for the discovery and identification reaches on the individual Z' models at the ILC; and finally, Sec. 5 contains some concluding remarks.

2 Polarized observables and Z' models

The analysis at the ILC is somewhat different from the corresponding studies of Drell-Yan processes at the LHC. Deviations of the various observables from SM predictions, such as cross sections and asymmetries, due to the interference of the SM amplitude with s-channel exchanges of the Z', graviton resonance G or sneutrino $\tilde{\nu}$, might be observed at the ILC. However, in the latter case, there is no interference of $\tilde{\nu}$ with the SM exchanges [5]. Conversely, in the case of the spin-2 KK graviton exchange, the interference with the SM exchanges vanishes when one integrates over the full angular range [26], whereas for differential observables such interference survives. Nevertheless, it turns out [27] that the sensitivity at the ILC with $\sqrt{s} = 0.5$ TeV and $\mathcal{L}_{\rm int} = 500$ fb^{-1} to a KK graviton resonance in processes (1) is of the order 0.8 TeV (1.9 TeV) for the graviton coupling constant $c = 0.01$ ($c = 0.1$), which is well within the expectations for discovery *and* identification at the LHC. Accordingly, the KK excitation would have been either discovered or excluded by the time the ILC will be operating. Therefore, from the considerations above, one can conclude that for $\sqrt{s} < M_{Z'}$, as will be the case for the ILC, only the interference of the Z' amplitude with the SM one could be visible at the ILC in processes (1). Accordingly, it

might not be so indispensible to perform angular analyses such as those foreseen for Drell-Yan processes at the LHC, in order to differentiate the spin of the exchanged intermediate heavy quantum states, because only Z' should be able to lead to appreciable interference effects.

The polarized differential cross section for the Bhabha process $e^+ + e^- \to e^+ + e^-$, where γ and Z can be exchanged also in the t-channel, can be written at leading order as (see, e.g., Refs. [28, 29]):

$$\begin{aligned}\frac{\mathrm{d}\sigma(P^-,P^+)}{\mathrm{d}z} &= \frac{(1+P^-)\,(1-P^+)}{4}\,\frac{\mathrm{d}\sigma_{\mathrm{R}}}{\mathrm{d}z} + \frac{(1-P^-)\,(1+P^+)}{4}\,\frac{\mathrm{d}\sigma_{\mathrm{L}}}{\mathrm{d}z} \\ &+ \frac{(1+P^-)\,(1+P^+)}{4}\,\frac{\mathrm{d}\sigma_{\mathrm{RL},t}}{\mathrm{d}z} + \frac{(1-P^-)\,(1-P^+)}{4}\,\frac{\mathrm{d}\sigma_{\mathrm{LR},t}}{\mathrm{d}z}, \end{aligned} \tag{2}$$

with the decomposition

$$\frac{\mathrm{d}\sigma_{\mathrm{L}}}{\mathrm{d}z} = \frac{\mathrm{d}\sigma_{\mathrm{LL}}}{\mathrm{d}z} + \frac{\mathrm{d}\sigma_{\mathrm{LR},s}}{\mathrm{d}z}, \qquad \frac{\mathrm{d}\sigma_{\mathrm{R}}}{\mathrm{d}z} = \frac{\mathrm{d}\sigma_{\mathrm{RR}}}{\mathrm{d}z} + \frac{\mathrm{d}\sigma_{\mathrm{RL},s}}{\mathrm{d}z}. \tag{3}$$

In Eqs. (2) and (3), the subscripts t and s denote helicity cross sections with SM γ and Z exchanges in the corresponding channels, $z = \cos\theta$ and the subscripts L, R denote the respective helicities, P^- and P^+ denote the degrees of longitudinal polarization of the e^- and e^+ beams, respectively.[1] In terms of helicity amplitudes:

$$\begin{aligned}\frac{\mathrm{d}\sigma_{\mathrm{LL}}}{\mathrm{d}z} &= \frac{2\pi\alpha^2_{\mathrm{e.m.}}}{s}\left|G^{ee}_{\mathrm{LL},s} + G^{ee}_{\mathrm{LL},t}\right|^2, \qquad \frac{\mathrm{d}\sigma_{\mathrm{RR}}}{\mathrm{d}z} = \frac{2\pi\alpha^2_{\mathrm{e.m.}}}{s}\left|G^{ee}_{\mathrm{RR},s} + G^{ee}_{\mathrm{RR},t}\right|^2, \\ \frac{\mathrm{d}\sigma_{\mathrm{LR},t}}{\mathrm{d}z} &= \frac{\mathrm{d}\sigma_{\mathrm{RL},t}}{\mathrm{d}z} = \frac{2\pi\alpha^2_{\mathrm{e.m.}}}{s}\left|G^{ee}_{\mathrm{LR},t}\right|^2, \quad \frac{\mathrm{d}\sigma_{\mathrm{LR},s}}{\mathrm{d}z} = \frac{\mathrm{d}\sigma_{\mathrm{RL},s}}{\mathrm{d}z} = \frac{2\pi\alpha^2_{\mathrm{e.m.}}}{s}\left|G^{ee}_{\mathrm{LR},s}\right|^2. \end{aligned} \tag{4}$$

According to the previous considerations the amplitudes $G^{ee}_{\alpha\beta,i}$, with $\alpha,\beta = \mathrm{L},\mathrm{R}$ and $i = s,t$, are given by the sum of the SM γ, Z exchanges plus deviations representing the effect induced by a Z' boson:

$$\begin{aligned} G^{ee}_{\mathrm{LL},s} &= u\left(\frac{1}{s} + \frac{(g^e_{\mathrm{L}})^2}{s-M_Z^2} + \frac{(g^{e\prime}_{\mathrm{L}})^2}{s-M_{Z'}^2}\right), \qquad G^{ee}_{\mathrm{LL},t} = u\left(\frac{1}{t} + \frac{(g^e_{\mathrm{L}})^2}{t-M_Z^2} + \frac{(g^{e\prime}_{\mathrm{L}})^2}{t-M_{Z'}^2}\right), \\ G^{ee}_{\mathrm{RR},s} &= u\left(\frac{1}{s} + \frac{(g^e_{\mathrm{R}})^2}{s-M_Z^2} + \frac{(g^{e\prime}_{\mathrm{R}})^2}{s-M_{Z'}^2}\right), \qquad G^{ee}_{\mathrm{RR},t} = u\left(\frac{1}{t} + \frac{(g^e_{\mathrm{R}})^2}{t-M_Z^2} + \frac{(g^{e\prime}_{\mathrm{R}})^2}{t-M_{Z'}^2}\right), \\ G^{ee}_{\mathrm{LR},s} &= t\left(\frac{1}{s} + \frac{g^e_{\mathrm{R}}\,g^e_{\mathrm{L}}}{s-M_Z^2} + \frac{g^{e\prime}_{\mathrm{R}}\,g^{e\prime}_{\mathrm{L}}}{s-M_{Z'}^2}\right), \qquad G^{ee}_{\mathrm{LR},t} = s\left(\frac{1}{t} + \frac{g^e_{\mathrm{R}}\,g^e_{\mathrm{L}}}{t-M_Z^2} + \frac{g^{e\prime}_{\mathrm{R}}\,g^{e\prime}_{\mathrm{L}}}{t-M_{Z'}^2}\right). \end{aligned} \tag{5}$$

Here, $u, t = -s(1 \pm z)/2$ (we are neglecting fermion masses), $g_{\mathrm{L}} = -\cot 2\,\theta_W$ and $g_{\mathrm{R}} = \tan\theta_W$ with θ_W the electroweak mixing angle, whereas g'_{L} and g'_{R} are characteristic of the particular Z' model. In the annihilation channel, below the Z' mass, the Z' interference with the SM will be destructive in the LL and RR cross sections, whereas it can be of either sign in the LR and RL cross sections.

The polarized differential cross section for the leptonic channels $e^+e^- \to l^+l^-$ with $l = \mu, \tau$ can be obtained directly from Eq. (2), basically by dropping the t-channel contributions. The same is true, after some obvious substitutions, for the annihilations into $c\bar{c}$ and $b\bar{b}$ final states, in which case also the color (N_C) and QCD correction factors,

[1] In the recent review [19], the opposite sign convention for positron polarization was adopted.

$C_s \simeq N_C\,[1+\alpha_s/\pi+1.4\,(\alpha_s/\pi)^2]$, must be taken into account. The s-channel helicity amplitudes for the process (1) with $f \neq e, t$ can be written as [28]:

$$G^{ef}_{\alpha\alpha,s} = u\left(\frac{Q_e\,Q_f}{s}+\frac{g^e_\alpha g^f_\alpha}{s-M_Z^2}+\frac{g'^e_\alpha g'^f_\alpha}{s-M_{Z'}^2}\right),\quad G^{ef}_{\alpha\beta,s} = t\left(\frac{Q_e\,Q_f}{s}+\frac{g^e_\alpha g^f_\beta}{s-M_Z^2}+\frac{g'^e_\alpha g'^f_\beta}{s-M_{Z'}^2}\right), \tag{6}$$

where in the latter expression $\alpha \neq \beta$.

As anticipated, the Z' models that will be considered in our analysis are the following:

(i) The Z' scenarios originating from the exceptional group E_6 spontaneous breaking are defined in terms of a mixing angle β. The specific values $\beta = 0$, $\beta = \pi/2$ and $\beta = -\arctan\sqrt{5/3}$, correspond to different E_6 breaking patterns and define the popular scenarios Z'_χ, Z'_ψ and Z'_η, respectively.

(ii) The left-right models, originating from the breaking of an $SO(10)$ grand-unification symmetry, and where the corresponding $Z'_{\rm LR}$ couples to a combination of right-handed and $B-L$ neutral currents (B and L denote baryon and lepton currents), specified by a real parameter $\alpha_{\rm LR}$ bounded by $\sqrt{2/3} \lesssim \alpha_{\rm LR} \lesssim \sqrt{2}$. The particular value $\alpha_{\rm LR} = \sqrt{2}$ corresponds to a pure L-R symmetric model (LRS).

(iii) The $Z'_{\rm ALR}$ predicted by the 'alternative' left-right scenario.

(iv) The so-called sequential $Z'_{\rm SSM}$, where the couplings to fermions are the same as those of the SM Z.

Detailed descriptions of these models, as well as the specific references, can be found, e. g., in Ref. [1]. All numerical values of the Z' couplings needed in Eq. (5) are collected, for example, in Table 1 of Ref. [14].

3 Discovery of Z'

In the absence of available data, the assessment of the expected 'discovery reaches' on the various Z's needs the definition of a 'distance' between the NP model predictions and those of the SM for the basic observables that will be measured. The former predictions parametrically depend on the Z' mass and its corresponding coupling constants, while the latter ones are calculated using the parameters known from the SM fits. Such a comparison can be performed by a standard χ^2-like procedure. As anticipated in Sec. 1, we divide the full angular range into bins and identify the basic observables with the polarized differential angular distributions for processes (1), $\mathcal{O} = {\rm d}\sigma(P^-,P^+)/{\rm d}z$, in each bin. Correspondingly, the relevant χ^2 can symbolically be defined as:

$$\chi^2(\mathcal{O}) = \sum_f \sum_{\{P^-,\,P^+\}} \sum_{\rm bins} \frac{[\mathcal{O}({\rm SM}+Z') - \mathcal{O}({\rm SM})]^2_{\rm bin}}{\left(\delta\mathcal{O}_{\rm bin}\right)^2}. \tag{7}$$

Notice that not only the different beam longitudinal polarizations, but eventually also the various processes 'f' in Eq. (1) are combined in the definition (7). Here, one assumes to have produced a set of 'data', for example by using the dynamics specified by

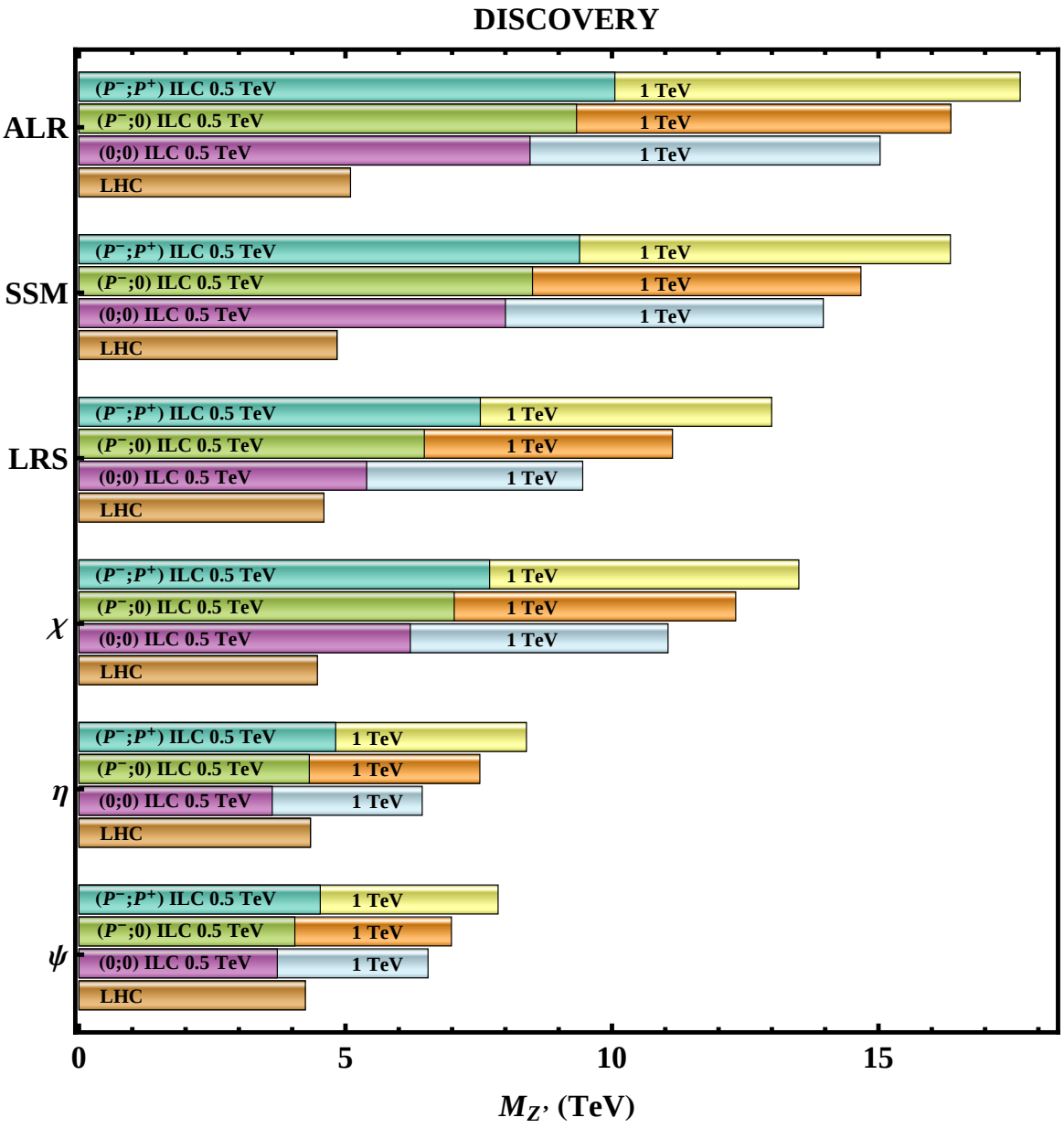

Figure 1: Discovery reaches on Z' models obtained from combined analysis of the unpolarized and polarized processes (1) (95% C.L.) at the ILC with $\sqrt{s} = 0.5$ TeV (1 TeV) and $\mathcal{L}_{\rm int} = 500$ fb^{-1} (1000 fb^{-1}), compared to the results expected from Drell-Yan processes at the LHC at the 5-σ level [14]. Three options of polarization are considered at the ILC: unpolarized beams, $P^- = P^+ = 0$; polarized electron beam, $|P^-| = 0.8$; both beams polarized, $|P^-| = 0.8$ and $|P^+| = 0.6$.

a given Z' model, and $\delta\mathcal{O}$ in the denominator denotes the corresponding 'experimental' uncertainty on $\mathcal{O}$, combining statistical and, if possible, systematical ones. According to the previous considerations, the χ^2, besides the number of degrees of freedom, is basically a function of the chosen Z' model parameters. In particular, if the coupling constants are fixed at specific values, it will depend solely on the Z' mass, and we vary this parameter. The discovery sensitivity to the Z' under consideration can in this case be identified as the limiting value of $M_{Z'}$ for which the value of $\chi^2(M_{Z'})$ has the probability needed for *exclusion* of the SM at a desired confidence level (in what follows, we shall impose 95% C.L.). In the cases where $\cos\beta$- or $\alpha_{\rm LR}$-dependent couplings are considered, SM *exclusion* regions can be defined analogously.

To derive the expected 'discovery' limits on Z' models at the ILC, for the 'annihilation' channels in Eq. (1), with $f \neq e, t$, we restrict ourselves to combining in Eq. (7) the $(P^-, P^+) = (|P^-|, -|P^+|)$ and $(-|P^-|, |P^+|)$ beam polarization configurations, that are the predominant ones. For the Bhabha process, $f = e$, we combine in (7) the cross sections with all four possible polarization configurations, i.e., $(P^-, P^+) = (|P^-|, -|P^+|)$, $(-|P^-|, |P^+|)$, $(|P^-|, |P^+|)$, $(-|P^-|, -|P^+|)$. Numerically, following the ILC Design Report [17], we take for the electron beam $|P^-| = 0.8$. For the positron beam, $|P^+| = 0.3$ is discussed as possibly available 'free of charge' already in the ILC initial running conditions. However, such a small positron polarization will turn out not to affect our evaluated discovery and identification reaches on Z's considerably. We shall therefore present numerical results for two cases, unpolarized positron beam $|P^+| = 0$, and $|P^+| = 0.6$ representing the 'ultimate' upgrade.

Regarding the ILC energy and the time-integrated luminosity (which, for simplicity, we assume to be equally distributed among the different polarization configurations defined above), still according to Ref. [17], we will give explicit numerical results for c.m. energy $\sqrt{s} = 0.5$ TeV with time-integrated luminosity $\mathcal{L}_{\rm int} = 500\ {\rm fb}^{-1}$, and for the 'ultimate' upgrade values $\sqrt{s} = 1.0$ TeV with $\mathcal{L}_{\rm int} = 1000\ {\rm fb}^{-1}$. The assumed final state identification efficiencies governing, together with the luminosity, the expected statistical uncertainties, are: 100% for e^+e^- pairs; 95% for l^+l^- events ($l = \mu, \tau$); 35% and 60% for $c\bar{c}$ and $b\bar{b}$, respectively [17, 18].

As for the major systematic uncertainties, they originate from errors on beam polarizations, on the time-integrated luminosity, and the final-state reconstruction and energy efficiencies. For the longitudinal polarizations, we adopt the values $\delta P^-/P^- = \delta P^+/P^+ = 0.25\%$, rather ambitious, especially as far as P^+ is concerned, but strictly needed for conducting the planned measurements at the permille level, see, e.g., Refs. [30–32].[2] As regards the other systematic uncertainties mentioned above, we assume for the combination the (perhaps conservative) lumpsum value of 0.5%. The systematic uncertainties are included using the covariance matrix approach [33–35].

Concerning the theoretical inputs, for the SM amplitudes we use the effective Born approximation [36] vertices, with $m_{\rm top} = 175$ GeV and $m_{\rm H} = 120$ GeV. The numerically dominant $\mathcal{O}(\alpha)$ QED corrections are generated by initial-state radiation, for both Bhabha scattering and the annihilation processes in (1). They are accounted for by a structure function approach including both hard and soft photon emission [37], and by a flux factor method [38], respectively. Effects of radiative flux return to the s-channel Z exchange are

[2] For simplicity we here assume equal precisions on beam polarizations. Clearly, much larger systematic errors on P^+ could partially spoil the advantages expected from the availability of also positron beam polarization.

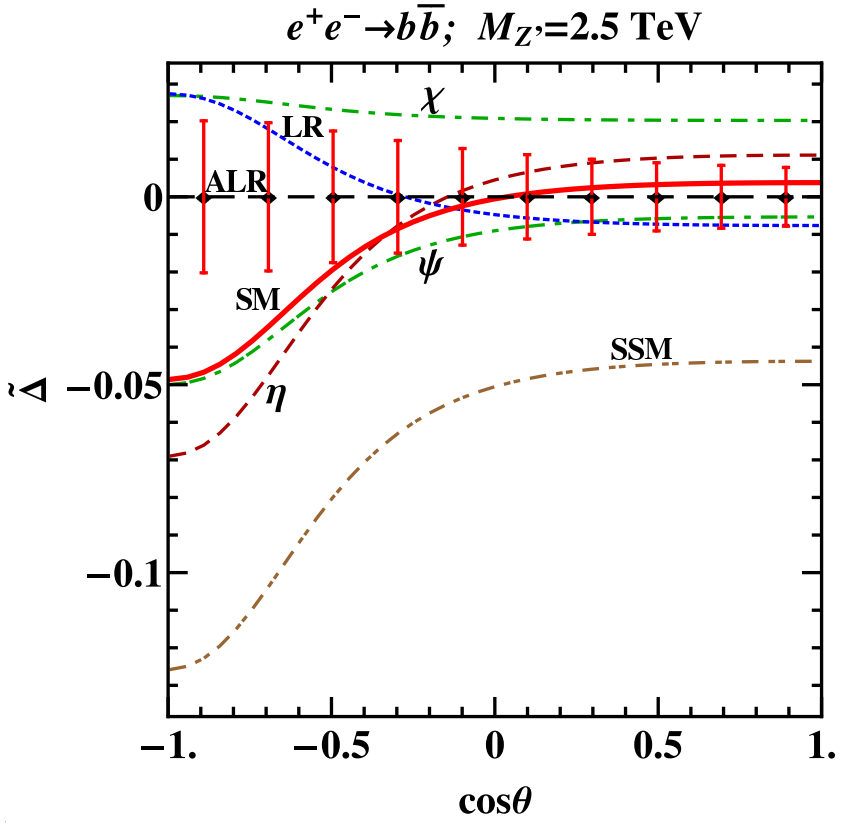

Figure 2: Relative deviation of the unpolarized differential cross sections from the ALR-model prediction $\tilde{\Delta}$ for the process $e^+e^- \to b\bar{b}$ as a function of $\cos\theta$ for the SM and considered Z' models with $M_{Z'} = 2.5$ TeV at the ILC with $\sqrt{s} = 0.5$ TeV and $\mathcal{L}_{\rm int} = 500$ fb^{-1}. The error bars are statistical uncertainties at the 1-σ level.

minimized by the cut $\Delta \equiv E_\gamma/E_{\rm beam} < 1 - M_Z^2/s$ on the radiated photon energy, with $\Delta = 0.9$. In this way, only interactions that occur close to the nominal collider energy are included in the analysis and, accordingly, the sensitivity to the manifestations of the searched-for nonstandard physics can be optimized. By numerical studies based on the ZFITTER code [39], other QED effects such as final-state and initial-final state emission are found, in the processes $e^+e^- \to l^+l^-$ ($l = \mu, \tau$) and $e^+e^- \to q\bar{q}$ ($q = c, b$), to be numerically unimportant for the chosen kinematical cuts. Finally, correlations between the different polarized cross sections (but not between the individual angular bins) are taken into account in the derivation of the numerical results, that we present in Fig. 1. The figure includes a comparison with the discovery potential of the LHC with luminosity 100 fb^{-1}, from the Drell-Yan processes $pp \to l^+l^- + X$ ($l = e$, μ) (at the 5-σ level). These values provide a representative overview of the sensitivities of the reach in $M_{Z'}$ on the planned energy and luminosity, as well as on beam polarization.

4 Distinction of Z' models

Basically, in the previous subsection we have assessed the extent to which Z' models can give values of e^+e^- differential cross sections that can *exclude* the SM hypothesis to a prescribed C.L. Such 'discovery reaches' are represented by upper limits on Z' masses, for

which the observable deviations between the corresponding Z' models and SM predictions are sufficiently large compared to the foreseeable experimental uncertainties on the cross sections at the ILC.

However, since different models can give rise to similar deviations, we would like to determine the ILC potential of identifying, among the various competing possibilities, the source of a deviation, should it be effectively observed. These ID-limits should obviously be expected to lie below the corresponding ILC discovery reaches and, for an approximate but relatively simple assessment, we adapt the naive χ^2-like procedure applied in the previous subsection.

To this purpose, we start by defining a 'distance' between pairs of Z' models, i and j with i, j denoting any of the SSM, SM, ALR, LRS, ψ, η, χ, but $i \neq j$. We assume for example model i to be the 'true' model, namely, we consider 'data' sets obtained from the dynamics i, with corresponding 'experimental' uncertainties, compatible with the expected 'true' experimental data. The assessment of its distinguishability from a j model, that we call 'tested' model, can be performed by a χ^2 comparison analogous to (7), with the χ^2 defined as:

$$\chi^2(\mathcal{O})_{i,j} = \sum_f \sum_{\{P^-,\ P^+\}} \sum_{\text{bins}} \frac{\left[\mathcal{O}(Z'_i) - \mathcal{O}(Z'_j)\right]^2_{\text{bin}}}{\left(\delta_i \mathcal{O}_{\text{bin}}\right)^2}. \tag{8}$$

As an illustration, the angular behavior of the deviations in the numerator of Eq. (8) for the unpolarized annihilation $e^+e^- \to b\bar{b}$ is depicted in Fig. 2, for the case where the 'true' model is i = ALR, with $M_{Z'} = 2.5$ TeV for all models, at the ILC with $\sqrt{s} = 0.5$ TeV and $\mathcal{L}_{\text{int}} = 500$ fb^{-1} (actually, in this figure, $\tilde{\Delta}$ is the relative deviation, $\tilde{\Delta} = \mathrm{d}\sigma(Z'_{ALR})/\mathrm{d}\sigma(Z'_j) - 1$).

Basically, considering that the ILC will start when the LHC will already be operating at the design energy and luminosity, as anticipated previously, we can envisage two cases requiring somewhat different strategies.

4.1 Z' mass known

In the first case we assume that the Z' mass is already measured at the LHC, but perhaps not 'identified' there, and the value is within the ILC discovery reaches for both models i and j. In this case one should set $M_{Z'_i} = M_{Z'_j} \equiv M_{Z'}$ in Eq. (8) and, accordingly, the χ^2 becomes a function of only the Z'_i and Z'_j coupling constants. If both the Z'_i and Z'_j couplings are fixed numerically, like in the example of Fig. 2, distinguishability can be assessed by varying $M_{Z'}$, up to the point where the χ^2_{ij} reaches the critical value suitable for *exclusion* of the 'tested' model j by the 'true' model i at the desired confidence level.

If the above mentioned couplings are, instead, the β- or α_{LR}- dependent ones, 'confusion' domains between 'true' and 'tested' models can analogously be determined by means of Eq. (8) in the model parameter plane $(\cos\beta, \alpha_{\text{LR}})$ for fixed values of $M_{Z'_i} = M_{Z'_j} \equiv M_{Z'}$. By definition, in these 'confusion' domains, that depend on the actual value assumed for $M_{Z'}$, the cross sections corresponding to definite values of β and α_{LR} cannot be distinguished from each other at the desired confidence level. Correspondingly, the 'complementary' regions in the above mentioned parameter plane can define the 'resolution' domain of the 'tested' model by the the 'true' model hypothesis, and determine in this way the identification limit on the latter.

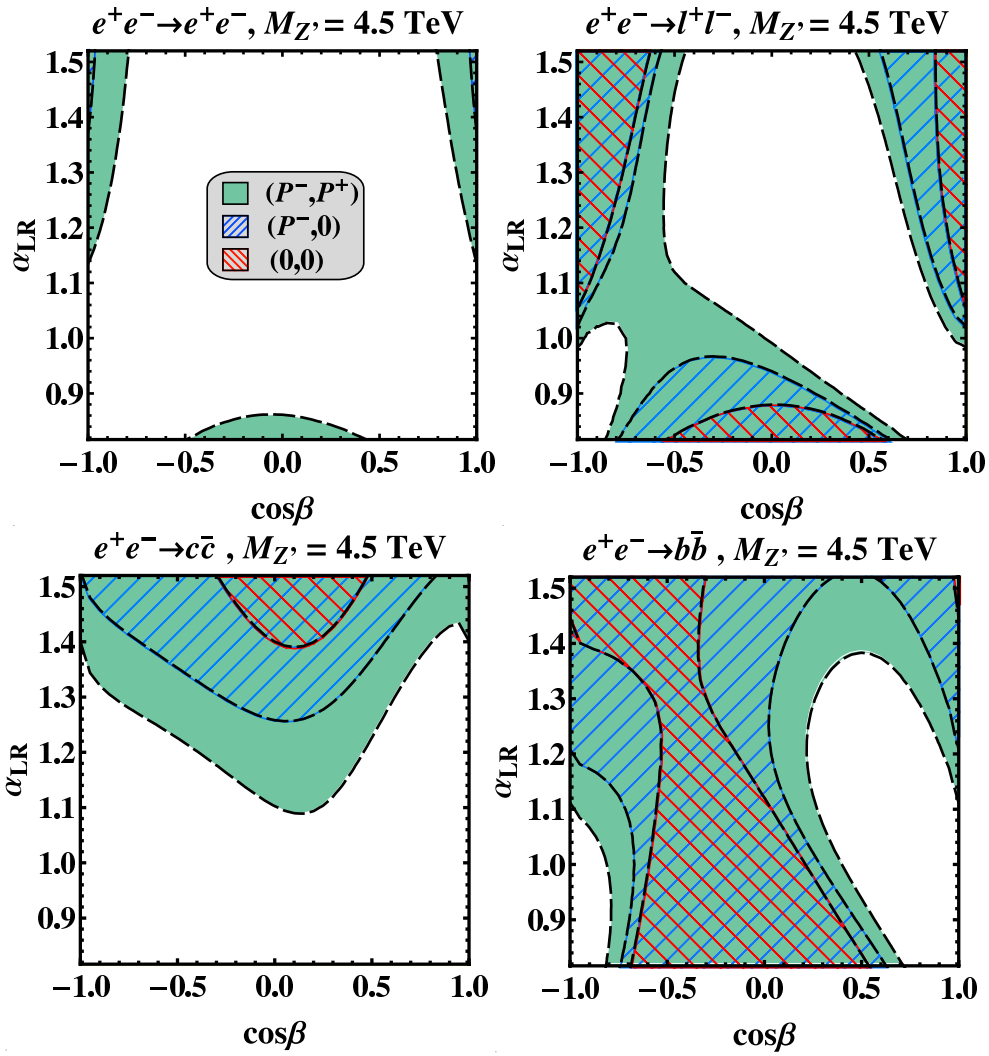

Figure 3: Regions of resolution (red hatched) of E_6 vs. left-right LR models in the model parameter plane $(\cos\beta, \alpha_{\rm LR})$ for $M_{Z'} = 4.5$ TeV obtained with Eq. (8) from the processes with different final states $e^+e^- \to e^+e^-$, l^+l^- $(l = \mu,\, \tau)$ $c\bar{c}$, $b\bar{b}$, at $\sqrt{s} = 0.5$ TeV, $\mathcal{L}_{\rm int} = 500$ fb^{-1}. The role of polarization is demonstrated. Using also a polarized electron (and positron) beam, the resolution region would enlarge to include also the blue hatched (plus the shaded, unhatched) regions, but not the white ones. Those would remain as 'confusion' regions.

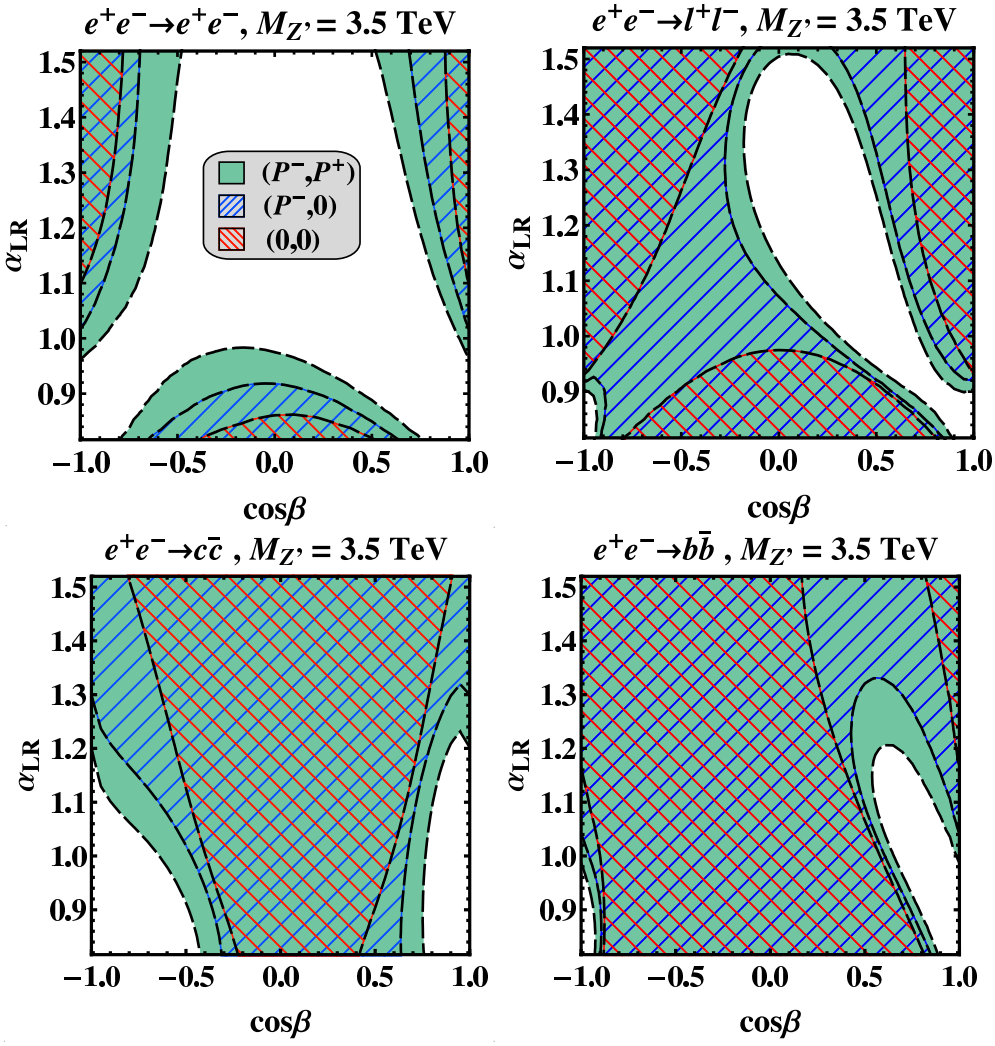

Figure 4: Similar to Fig. 3 but for $M_{Z'} = 3.5$ TeV.

As an illustrative example of application of the ID-criteria exposed above, we evaluate the 'resolution' regions between E_6 ('true') and left-right LR ('tested') models in the plane $(\cos\beta, \alpha_{\rm LR})$ for different values of $M_{Z'}$. Figures 3-6 show the regions of 'resolution' obtained from the processes $e^+e^- \to e^+e^-$, l^+l^- $(l = \mu,\, \tau)$, $c\bar{c}$ and $b\bar{b}$, for $M_{Z'}$ =4.5 TeV, 3.5 TeV and 2.5 TeV at $\sqrt{s} = 0.5$ TeV and $\mathcal{L}_{\rm int} = 500$ fb^{-1}, and for different values of beam polarization. Notice that, in these figures, the horizontal axis includes also the values of β specific of the χ, ψ and η models, while the vertical axis includes the value of $\alpha_{\rm LR}$ representative of the LRS model.[3]

Figures 3–5 clearly demonstrate the complementary roles of the processes with different final states, in particular, that the process $e^+e^- \to b\bar{b}$ can potentially be the most efficient one in distinguishing E_6 and left-right models from each other (it provides the largest resolution domains). Conversely, the purely leptonic processes, $f = e,\, \mu,\, \tau$ in (1), turn out to determine much less extended 'resolution' areas, in particular they cannot discriminate

[3]Actually, we should recall that the point $(\cos\beta, \alpha_{\rm LR}) = (1, \sqrt{2/3})$ corresponds to the χ model which, indeed, exists in both classes of Z' models. Therefore, since one would be testing the χ model against itself, that point must not be considered in an analysis based on Eq. (8).

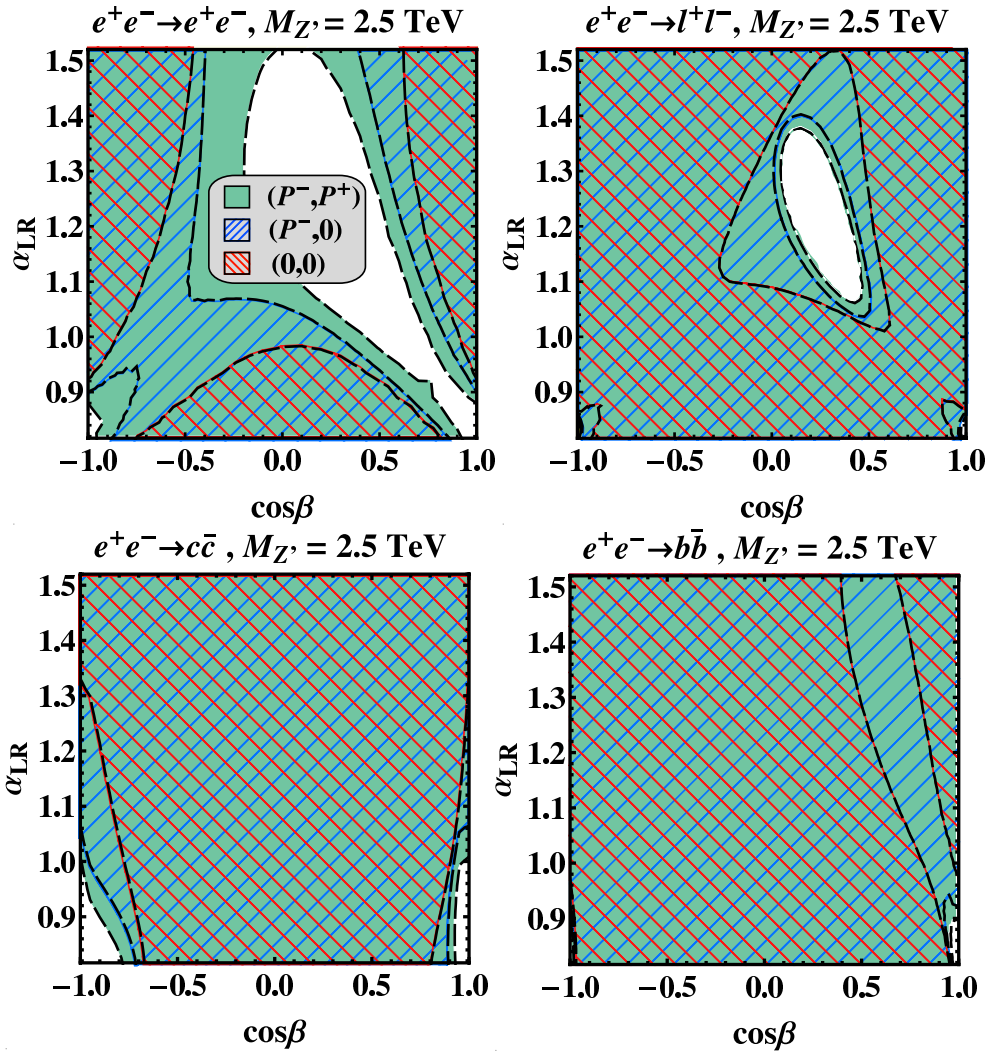

Figure 5: Similar to Fig. 3 but for $M_{Z'} = 2.5$ TeV.

the LR model from the E_6 models at $(\cos\beta, \alpha_{\rm LR}) = (\pm 1, \sqrt{2/3})$ and $(1/4, \sqrt{3/2})$ (for any $M_{Z'} > \sqrt{s}$).

Also, as can be seen from these figures, the leptonic processes are found to provide 'confusion' domains (white) located in the 'central' part of the plane $(\cos\beta, \alpha_{\rm LR})$, around $(1/4, \sqrt{3/2})$, whereas the processes into $q\bar{q}$ final states exhibit the opposite feature. Therefore, as shown in Fig. 6, the combination of all processes f is expected to dramatically reduce the 'confusion' area in the above mentioned plane and to determine the largest possible domain in which the considered Z' models can be mutually distinguished from one another. The substantial role of electron polarization and, to a somewhat lesser extent, of positron polarization in shrinking 'confusion' domains, leading to enlarged model 'resolution' domains, can also be seen in these panels. Combining all processes, and with both beams polarized, a 'confusion' turns out to persist only in the minute corners shown in Fig. 6, for $M_{Z'} = 4.5$ GeV, and nothing at the lower masses.

It is interesting to compare these resolution regions with the corresponding ones resulting from the assumed Z' discovery in the Drell-Yan process at the LHC, shown in the lower-right panel of Fig. 6. This figure shows that, at the LHC, for the discovery of

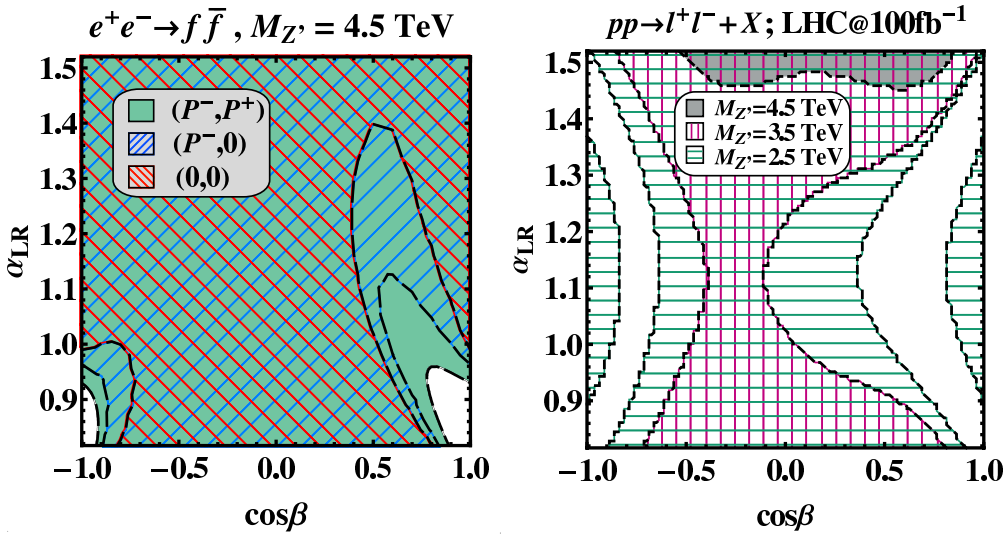

Figure 6: Left: Resolution domains at $M_{Z'} = 4.5$, exploiting all final states. Right: Corresponding resolution domains for Drell-Yan production at the LHC, for the three values of $M_{Z'}$.

a 4.5 TeV Z' the corresponding resolution region is found to cover only a narrow strip, $1.4 \lesssim \alpha_{\rm LR}$ and $-0.5 \lesssim \cos\beta \lesssim 0.8$. Even for $M_{Z'} = 2.5$ TeV, at the LHC, there are only modest hyperbola-like strips at $|\cos\beta| \gtrsim 0.5$ where models can be distinguished.

We now continue the above analysis in a somewhat different direction, namely, we wish to determine the limiting value of $M_{Z'}$ up to which a particular $\cos\theta$-dependent E_6 model, assumed to be true, can be identified at the ILC in the sense that all the other, potentially competing, Z' models can be excluded. The results from this analysis are shown in Figs. 7–9.

Figure 7 exhibits the exclusion limits vs. β on the models LR, ALR, SSM and SM (recall that exclusion of the SM determines the discovery reaches), once a E_6 model is 'true' (all processes combined). For the LR 'tested' model, the corresponding curve in Fig. 7 is obtained, for each β, by varying $\alpha_{\rm LR}$ in the full allowed range, which gives LR exclusion limits $M_{Z'}(\alpha_{\rm LR})$, and choosing the minimum value of such $M_{Z'}$s (in this way the *whole* class of LR models, as well as the LRS, are excluded). The solid line labelled 'SM' represents the discovery reach, i.e., the Z' mass up to which the SM can be excluded. The overall identification range is shown as the shaded (yellow) region. One can see that, in this case, the identification of the class of E_6 models considered here is basically determined by the exclusion of the class of the LR models and, for the 'central' values of $\cos\beta$, by the SM (i.e., by the discovery reach). Consequently the ID-limit is, in a (somewhat broad) range around $\cos\beta = 0$, essentially identical to the discovery limit, whereas it is substantially smaller in the two intervals close to $|\cos\beta| = 1$. Figure 7 shows that, numerically, for $|\cos\beta| < 0.9$ the ID-limit is as large as $M_{Z'}^{\rm ID} \simeq 3 - 4$ TeV, and for $\cos\beta$ near ± 1 E_6 models become more and more difficult to distinguish from the competitor ones. The right panel of Fig. 7 shows the corresponding identification reaches for the polarized case, $|P^-| = 0.8$ and $|P^+| = 0.6$, and the quantitative improvements that can be achieved in this case.

Similarly, the identification limits on LR models vs. the parameter $\alpha_{\rm LR}$ can be read off from Fig. 8. The curve labelled as 'E_6' is obtained by a procedure analogous to the

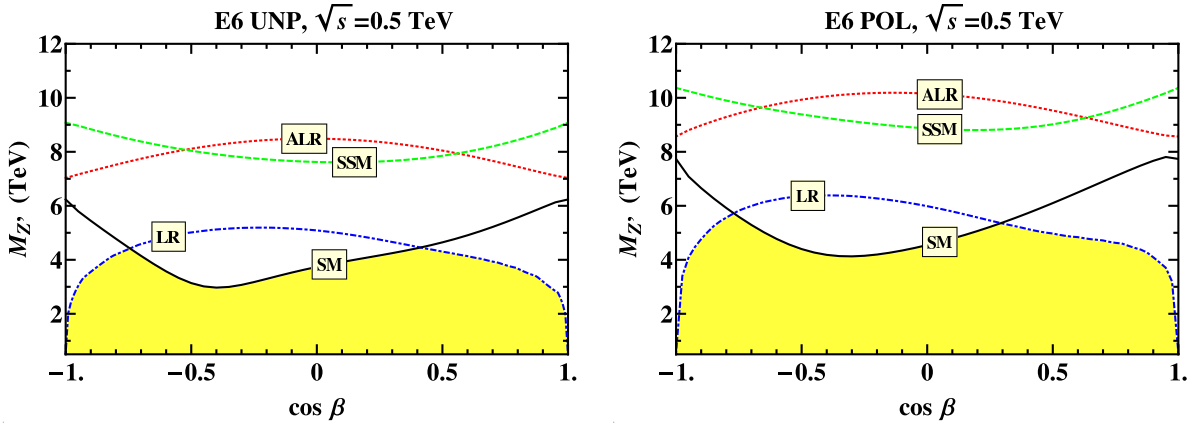

Figure 7: Left panel: E6 identification reaches on $M_{Z'}$ at 95% C.L. obtained from combination of all unpolarized processes $e^+e^- \to f\bar{f}$ at $\sqrt{s}$=0.5 TeV and $\mathcal{L}_{\rm int}$=500 fb^{-1}. The E_6 model is assumed to be 'true' while the others (SSM, LR, ALR, SSM and SM) are taken as tested models. The identification range is indicated as the shaded (yellow) area. Right panel: Similar, but for the polarized processes.

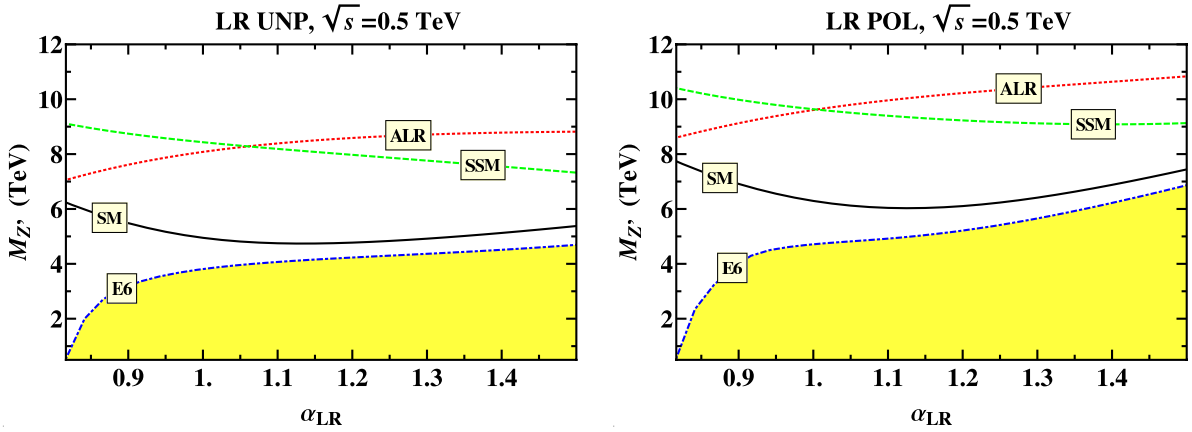

Figure 8: Similar to Fig. 7, for LR models.

curve 'LR' in Fig. 7, and the solid curve 'SM' represents the exclusion limits of the SM (hence the discovery reaches). In this case, the identification of the class of LR Z's turns out to be determined basically by the exclusion of the class of E_6 models, generally not so much below the discovery limit for all values of $\alpha_{\rm LR}$. On the other hand, the figure shows rather high identification limits, of the order of $M_{Z'}^{\rm ID} \simeq 3.0 - 4.6$ TeV in the range, say, $0.9 \lesssim \alpha_{\rm LR} \lesssim \sqrt{2}$, whereas they substantially decrease for smaller $\alpha_{\rm LR}$.

We can conclude, from Figs. 7 and 8, that the identification reach at the ILC, already at $\sqrt{s} = 0.5$ TeV and $\mathcal{L}_{\rm int}$=500 fb^{-1}, exceeds the corresponding discovery reach at the LHC. In fact, the full integrated luminosity considered here might be not quite indispensible for this identification. In Table 1 we show the required integrated luminosity, at the two ILC energies of 0.5 and 1 TeV, for the identification of these different models, realized as a Z' at 2.5, 3.5 or 4.5 TeV (within the discovery reach of the LHC).

Finally, in Fig. 9 we summarize the information, of a similar kind as represented in Figs. 7 and 8, relevant to the cases where the ALR model or the SSM model is assumed 'true' (upper and lower panels, respectively). As usual, the figure shows the limiting value

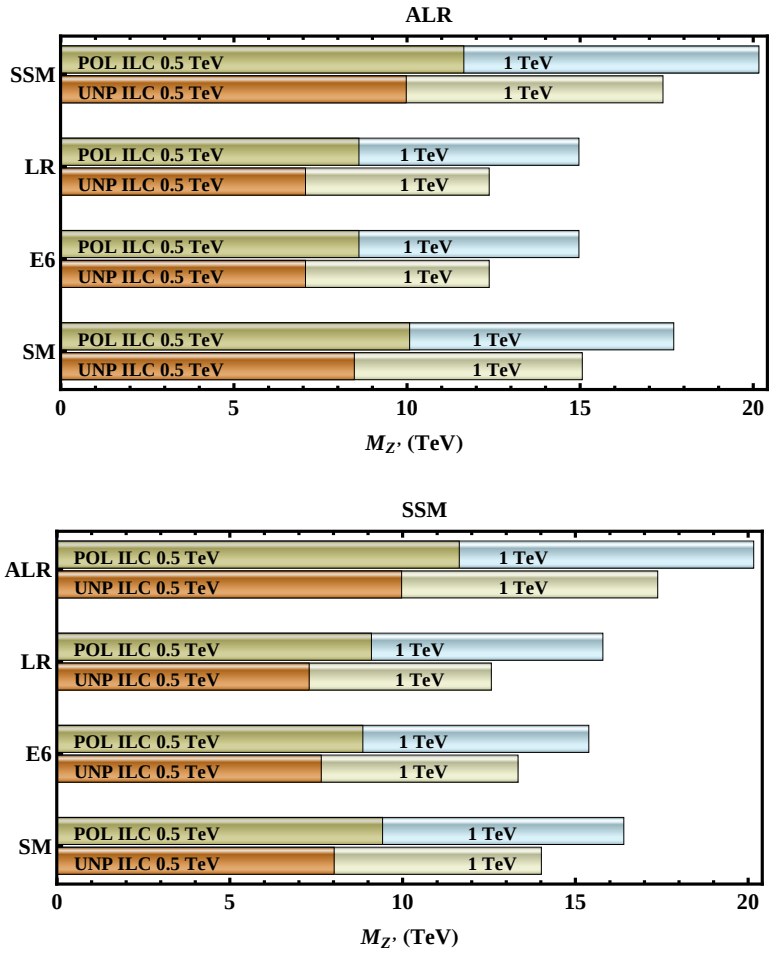

Figure 9: Exclusion reaches on $M_{Z'}$ at 95% C.L. obtained from combination of all processes $e^+e^- \to f\bar{f}$ at $\sqrt{s}$=0.5 (1.0) TeV and $\mathcal{L}_{\rm int}$=500 (1000) fb^{-1} in the case when the ALR model (top panel) or SSM model (bottom) is assumed to be the 'true' models while the others are taken as tested models. The unpolarized and polarized cases are compared.

Table 1: Required integrated luminosity, $\mathcal{L}_{\rm int}$[fb^{-1}], at the two energies $\sqrt{s}$ = 0.5 and 1 TeV and with polarized beams, required for model identification. Three mass values, $M_{Z'}$ = 2.5 TeV, 3.5 TeV and 4.5 TeV, assumed determined at the LHC, are considered.

$\sqrt{s}$	E6			LR			ALR			SSM		
	2.5	3.5	4.5	2.5	3.5	4.5	2.5	3.5	4.5	2.5	3.5	4.5
0.5 TeV	49.6	225	785	51.0	241	944	2.3	9.4	27.1	2.1	8.5	24.0
1 TeV	9.1	41.6	125	9.4	42.3	128	0.4	2.0	5.9	0.4	1.8	5.3

of $M_{Z'}$ at which the other Z' models can be excluded, the SM being one of them. The two energies 0.5 TeV and 1 TeV are considered, the different processes (1) are combined in the χ^2, and the unpolarized and polarized cases ($|P^-| = 0.8$, $|P^+| = 0.6$) are compared. The entries for the LR and E_6 models in this figure refer to the worst case, i.e., similar to the procedures adopted for the 'LR' and 'E_6' curves in Figs. 7 and 8, adopting the lowest value of $M_{Z'}$ as β and $\alpha_{\rm LR}$ are varied, in order to represent a whole class of models.

Specifically, in Fig. 9, one can easily read off the identification reaches for ALR and SSM models at 0.5 TeV: $M^{\rm ID}_{Z'_{\rm ALR}}$ and $M^{\rm ID}_{Z'_{\rm SSM}}$ are both 8–9 TeV if polarization is available. In a sense, the ALR and SSM models are the most 'orthogonal' ones since, if either of them is assumed 'true', the other one can be excluded up to a really high value of $M_{Z'}$.

4.2 Z' mass not known

The second kind of situation is met in the case where the Z' mass cannot be known *a priori*, e.g., the Z' is too heavy to be discovered at the LHC [say, $M_{Z'}$ >4–5 TeV], but deviations from the SM predictions can still be observed at the ILC. Actually, models with different Z' masses and coupling constants can in principle be the source of a deviation from the SM predictions observed at the ILC. With the coupling constants held fixed numerically at the theoretical values pertinent to the Z'_i and Z'_j models under consideration, the χ^2_{ij} of Eq. (8) becomes a function of the two masses, $M_{Z'_i}$ and $M_{Z'_j}$, both assumed to lie in the respective ILC discovery ranges. In this case, one can derive a contour in the two-dimensional $(M_{Z'_i}, M_{Z'_j})$ plane where to each value of $M_{Z'_i}$ is associated a value $\overline{M}_{Z'_j}$ such that, for all $M_{Z'_j} > \overline{M}_{Z'_j}$, the value of χ^2_{ij} in (8) is consistent with 'confusion' of i and j at the desired confidence level. The region encircled by such a contour will be the 'confusion' (or 'no distinction') domain between the 'true' model i and the 'tested' model j and correspondingly, in the complementary domain the hypothesis j could be *excluded* if i is assumed to be 'true'. We refer to this latter, complementary, region as 'resolution' region.

One can iterate this procedure and generate pairwise 'confusion' and 'exclusion' regions in the two-dimensional planes of parameters for all models $j \neq i$. As will be illustrated graphically in the remaining part of the paper, a common feature of such 'exclusion' regions is that the relevant contours admit, for each j (and obviously fixed i) a minimum value $M^{(j)}_{Z'_i}$ such that, for any value $M_{Z'_i} < M^{(j)}_{Z'_i}$, the 'tested' model j can be *excluded* regardless of $M_{Z'_j}$. We finally assume, as identification limit on the i model at ILC, the smallest of the values $M^{(j)}_{Z'_i}$for $j \neq i$, for which *all* tested models will be excluded by the hypothesis of i being 'true'. Of course, such ID-value of $M_{Z'}$ should be smaller (or at most equal), than the ILC discovery reach on model i. This procedure can finally be iterated, in turn, to all the different Z' models and the assessment of corresponding ID-reaches. This naive χ^2 procedure can also be extended in a straightforward way to estimating exclusion ranges—and corresponding identification limits—in the cases where $\cos\beta$- and/or $\alpha_{\rm LR}$-dependent Z' models are considered in Eq. (8).

Examples of pairwise 'confusion' regions and corresponding contours, relevant to the Z' models chosen in Fig. 1, are shown in Fig. 10. In this figure, the various steps of the procedure outlined above, as well as the final derivation of the ID-limits, can easily be followed. As an example of how to read this figure, consider the hypothesis that the η model is 'true' (lower left panel), with $M_{Z'} = 6$ TeV. Then, if instead the ψ or χ model should be true, the mass would have to exceed 4.2 or 6.3 TeV, respectively.

Finally, Fig. 11 shows the comparison of identification reaches or distinction bounds on the Z'-models considered in Fig. 1, together with the corresponding bounds on $M_{Z'}$ obtained from the process $pp \to l^+l^- + X$ at the LHC with c.m. energy 14 TeV and time-integrated luminosity 100 fb^{-1}. We assume, for the ILC, the same c.m. energy, luminosty and beam polarization as in Fig. 1. The figure speaks for itself, and in particular

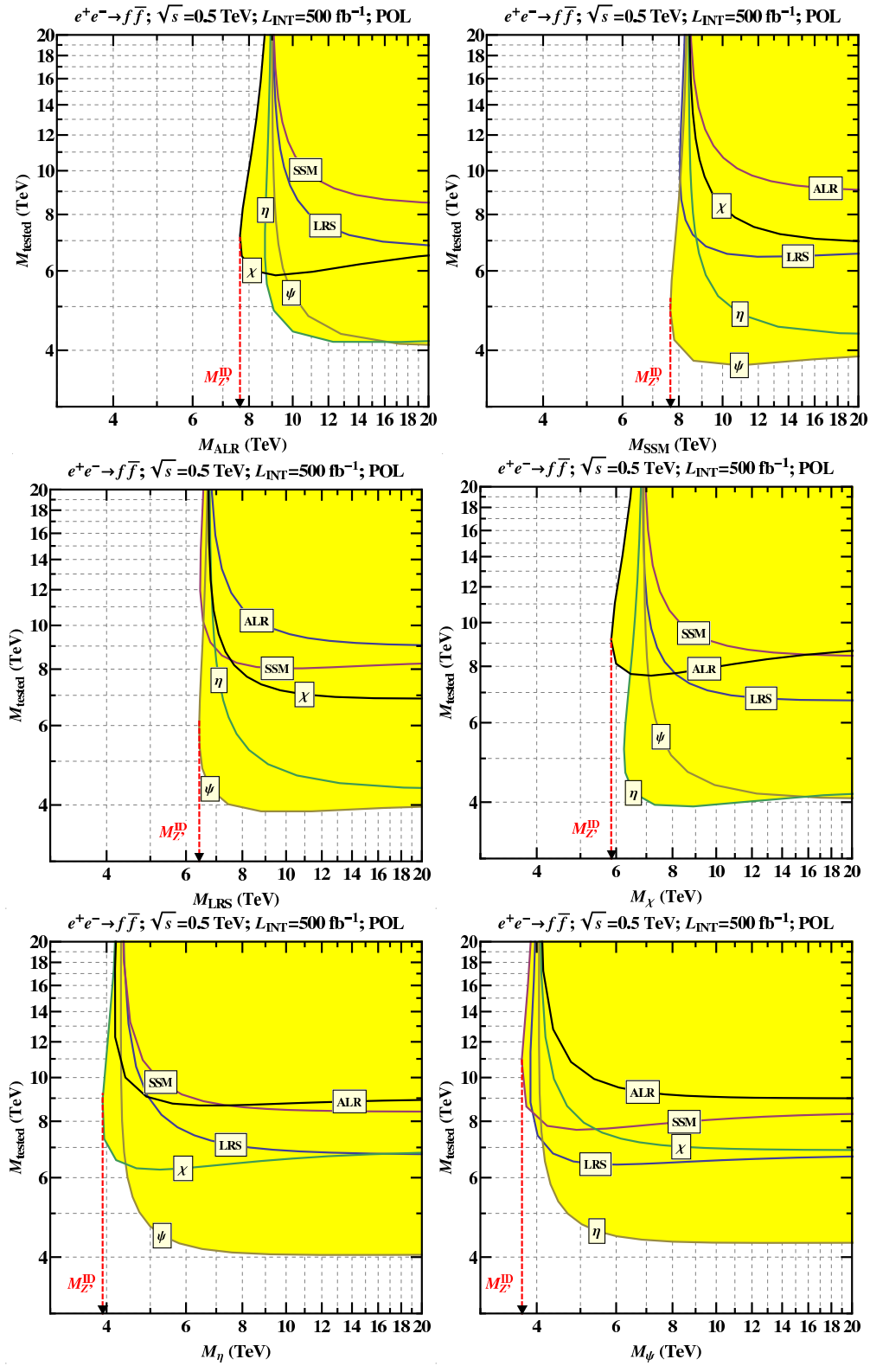

Figure 10: Regions of confusion (yellow shaded areas) between a 'true' Z' model and the 'tested' Z' models in the mass plane $(M_{\rm true}, M_{\rm tested})$ at 95% C.L. obtained from combination of all polarized processes $e^+e^- \to f\bar{f}$ at $\sqrt{s}$=0.5 TeV and $\mathcal{L}_{\rm int}$=500 fb^{-1}. The dashed lines indicate the identification reach.

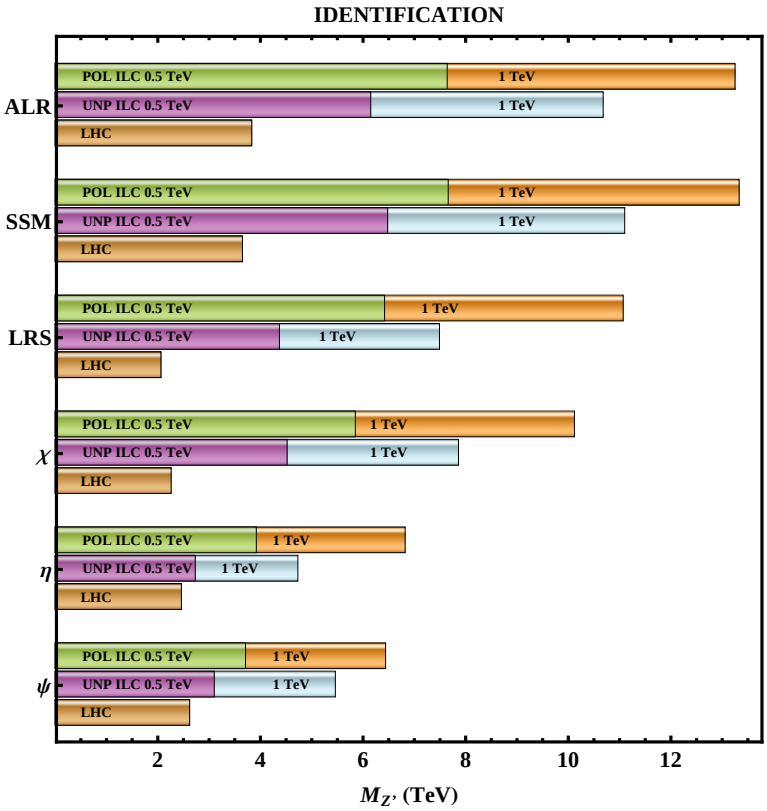

Figure 11: Comparison of the Z'-model distinction bounds on $M_{Z'}$ obtained from combined analysis of the unpolarized and polarized processes (1) at the ILC with $\sqrt{s} =$ 0.5 TeV (1 TeV) and $\mathcal{L}_{\rm int} = 500$ fb^{-1} (1000 fb^{-1}), compared to the results expected from Drell-Yan processes at the LHC at 95% C.L. [14]. Two options of polarization are considered: unpolarized beams $P^- = P^+ = 0$ and both beams are polarized, $|P^-| = 0.8$ and $|P^+| = 0.6$.

clearly exhibits the roles of the ILC parameters. In summary, one might be able to distinguish among the considered Z' models at 95% C.L. up to $M_{Z'} \simeq 3.1$ TeV (4.0 TeV) for unpolarized (polarized) beams at the ILC (0.5 TeV) and 5.3 TeV (7.0 TeV) at the ILC (1 TeV), respectively. In particular, the figure explicitly manifests the substantial role of electron beam polarization in sharpening the identification reaches. Positron polarization can also give a considerable enhancement in this regard (if measurable with the same high accuracy as for electron polarization), although to a more limited extent in some cases.

Clearly, our analysis is greatly simplified by the fact that the vector and axial vector couplings of the considered Z's are fixed theoretically. If we wanted to determine them in general, namely, with both masses *and* coupling constants *a priori* free variables, the χ^2 analysis should be five-dimensional with, in addition, the limitation that for $M_{Z'} \gg \sqrt{s}$ (contact-interaction regime), $M_{Z'}$ could not be simultaneously extracted. In principle, data at different collider energies could be utilized in this regard, for Z' masses not too far from $\sqrt{s}$ [40].

5 Concluding remarks

We have explored in some detail how the Z' discovery reach at the ILC depends on the c.m. energy, on the available polarization, as well as on the model actually realized in Nature. The lower part of this range, up to $M_{Z'} \simeq 5$ TeV, will also be covered by the LHC, but the identification reach at the LHC is only up to $M_{Z'} < 2.2$ TeV.

In this LHC discovery range, the cleaner ILC environment, together with the availability of beam polarization, allow for an identification of the particular Z' version realized. Actually, this ILC identification range extends considerably beyond the LHC discovery range. Specifically, the ILC with polarized beams at $\sqrt{s} = 0.5$ TeV and 1 TeV allows to identify all considered Z' bosons if $M_{Z'} \lesssim (6-7) \times \sqrt{s}$. This represents a substantial extension of the the LHC reach.

Acknowledgements
It is a great pleasure to thank Nello Paver for his contributions to this study, in particular his critical and constructive comments. This research has been partially supported by the Abdus Salam ICTP and the Belarusian Republican Foundation for Fundamental Research. The work of PO has been supported by the Research Council of Norway.

References

[1] For reviews and original references see, e.g., P. Langacker, arXiv:0801.1345 [hep-ph]; T. G. Rizzo, arXiv:hep-ph/0610104;
A. Leike, Phys. Rept. **317**, 143 (1999) [arXiv:hep-ph/9805494];
J. L. Hewett and T. G. Rizzo, Phys. Rept. **183**, 193 (1989).

[2] For recent constraints from electroweak data, see J. Erler, P. Langacker, S. Munir and E. R. Pena, JHEP **0908**, 017 (2009) [arXiv:0906.2435 [hep-ph]].

[3] T. Aaltonen *et al.* [CDF Collaboration], Phys. Rev. Lett. **99**, 171802 (2007) [arXiv:0707.2524 [hep-ex]]; Phys. Rev. Lett. **102**, 091805 (2009) [arXiv:0811.0053 [hep-ex]];
R. J. Hooper [D0 Collaboration], Int. J. Mod. Phys. A **20**, 3277 (2005).

[4] L. Randall and R. Sundrum, Phys. Rev. Lett. **83** (1999) 3370 [arXiv:hep-ph/9905221]; Phys. Rev. Lett. **83** (1999) 4690 [arXiv:hep-th/9906064].

[5] J. Kalinowski, R. Ruckl, H. Spiesberger and P. M. Zerwas, Phys. Lett. B **406** (1997) 314 [arXiv:hep-ph/9703436]; Phys. Lett. B **414** (1997) 297 [arXiv:hep-ph/9708272]; T. G. Rizzo, Phys. Rev. D **59** (1999) 113004 [arXiv:hep-ph/9811440].

[6] B. C. Allanach, K. Odagiri, M. A. Parker and B. R. Webber, JHEP **0009**, 019 (2000) [arXiv:hep-ph/0006114];
B. C. Allanach, K. Odagiri, M. J. Palmer, M. A. Parker, A. Sabetfakhri and B. R. Webber, JHEP **0212**, 039 (2002) [arXiv:hep-ph/0211205].

[7] M. Dittmar, A. S. Nicollerat and A. Djouadi, Phys. Lett. B **583**, 111 (2004) [arXiv:hep-ph/0307020].

[8] R. Cousins, J. Mumford, J. Tucker and V. Valuev, JHEP **0511**, 046 (2005).

[9] S. Godfrey, P. Kalyniak and A. Tomkins, arXiv:hep-ph/0511335; S. Godfrey and T. A. W. Martin, Phys. Rev. Lett. **101**, 151803 (2008) [arXiv:0807.1080 [hep-ph]]; R. Diener, S. Godfrey and T. A. W. Martin, arXiv:0910.1334 [hep-ph].

[10] D. Feldman, Z. Liu and P. Nath, JHEP **0611**, 007 (2006) [arXiv:hep-ph/0606294].

[11] F. Petriello and S. Quackenbush, Phys. Rev. D **77**, 115004 (2008) [arXiv:0801.4389 [hep-ph]]; Y. Li, F. Petriello and S. Quackenbush, Phys. Rev. D **80**, 055018 (2009) [arXiv:0906.4132 [hep-ph]].

[12] P. Osland, A. A. Pankov, N. Paver and A. V. Tsytrinov, Phys. Rev. D **78**, 035008 (2008) [arXiv:hep-ph/0805.2734], and arXiv:0902.1593 [hep-ph].

[13] H. Murayama and V. Rentala, arXiv:0904.4561 [hep-ph].

[14] P. Osland, A. A. Pankov, A. V. Tsytrinov and N. Paver, Phys. Rev. D **79**, 115021 (2009) [arXiv:0904.4857 [hep-ph]].

[15] E. Salvioni, G. Villadoro and F. Zwirner, arXiv:0909.1320 [hep-ph].

[16] T. G. Rizzo, JHEP **0908**, 082 (2009) [arXiv:0904.2534 [hep-ph]].

[17] J. Brau *et al.* [ILC Collaboration], "ILC Reference Design Report Volume 1 - Executive Summary," arXiv:0712.1950 [physics.acc-ph].

[18] G. Aarons *et al.* [ILC Collaboration], "International Linear Collider Reference Design Report Volume 2: PHYSICS AT THE ILC," arXiv:0709.1893 [hep-ph].

[19] G. A. Moortgat-Pick *et al.*, Phys. Rept. **460**, 131 (2008) [arXiv:hep-ph/0507011].

[20] M. Cvetic and S. Godfrey, "Discovery and identification of extra gauge bosons," arXiv:hep-ph/9504216;

[21] S. Riemann, LC report LC-TH-2001-007.

[22] A. Djouadi, A. Leike, T. Riemann, D. Schaile and C. Verzegnassi, Z. Phys. C **56**, 289 (1992).

[23] A. V. Gulov and V. V. Skalozub, Phys. Rev. D **70**, 115010 (2004) [arXiv:hep-ph/0408076].

[24] A. A. Pankov, N. Paver and A. V. Tsytrinov, Phys. Rev. D **73**, 115005 (2006) [arXiv:hep-ph/0512131].

[25] G. Weiglein *et al.* [LHC/LC Study Group], Phys. Rept. **426**, 47 (2006) [arXiv:hep-ph/0410364].

[26] J. L. Hewett, Phys. Rev. Lett. **82** (1999) 4765 [arXiv:hep-ph/9811356].

[27] H. Davoudiasl, J. L. Hewett and T. G. Rizzo, Phys. Rev. Lett. **84** (2000) 2080 [arXiv:hep-ph/9909255].

[28] B. Schrempp, F. Schrempp, N. Wermes and D. Zeppenfeld, Nucl. Phys. B **296**, 1 (1988).

[29] A. A. Pankov and N. Paver, Eur. Phys. J. C **29**, 313 (2003) [arXiv:hep-ph/0209058].

[30] S. Riemann, A. Schalicke and A. Ushakov, DESY 09-038, arXiv:0903.2366 [physics.ins-det].

[31] B. Aurand *et al.*, Report DESY-09-042, arXiv:0903.2959 [physics.acc-ph].

[32] S. Boogert *et al.*, ILC-NOTE-2009-049, arXiv:0904.0122 [physics.ins-det].

[33] W.T. Eadie, D. Drijard, F.E. James, M. Roos, B. Sadoulet, *Statistical methods in experimental physics* (American Elsevier, 1971).

[34] F. Cuypers and P. Gambino, Phys. Lett. B **388** (1996) 211 [hep-ph/9606391];
F. Cuypers, hep-ph/9611336.

[35] A. A. Babich, P. Osland, A. A. Pankov and N. Paver, Phys. Lett. B **518**, 128 (2001) [arXiv:hep-ph/0107159].

[36] M. Consoli, W. Hollik and F. Jegerlehner, CERN-TH-5527-89, *Presented at Workshop on Z Physics at LEP*;
G. Altarelli, R. Casalbuoni, D. Dominici, F. Feruglio and R. Gatto, Nucl. Phys. B **342**, 15 (1990).

[37] For reviews see, e.g., O. Nicrosini and L. Trentadue, in *Radiative Corrections for e^+e^- Collisions*, ed. J. H. Kühn 25 (Springer, Berlin, 1989), p. 25; in *QED Structure Functions, Ann Arbor, MI, 1989*, ed. G. Bonvicini, AIP Conf. Proc. No. 201 (AIP, New York, 1990), p. 12.

[38] For a review see, e.g., W. Benakker and F. A Berends: *Proc. of the Workshop on Physics at LEP2*, CERN 96-01, vol. 1, p. 79 and references therein.

[39] D. Y. Bardin, P. Christova, M. Jack, L. Kalinovskaya, A. Olchevski, S. Riemann and T. Riemann, Comput. Phys. Commun. **133**, 229 (2001) [arXiv:hep-ph/9908433].

[40] T. G. Rizzo, Phys. Rev. D **55**, 5483 (1997) [arXiv:hep-ph/9612304].